J Adv Manuf Eng, Vol. 5, Issue. 2, pp. 29–36, December, 2024

Journal of Advances in Manufacturing Engineering
Web page info: https://jame.yildiz.edu.tr
DOI: 10.14744/ytu.jame.2024.00005

Original Article

# Optimization of pre-turning parameters for diamond burnishing of AISI 4340 steel

**Mevlüt AYDIN***, **Ömer Faruk GÖKCEPINAR**, **Mete KALYONCU**

*Department of Mechanical Engineering, Konya Technical University, Konya, Türkiye*

## ARTICLE INFO

*Article history*
Received: 21 July 2024
Revised: 09 August 2024
Accepted: 19 August 2024

**Key words:**
Bees algorithm, diamond burnishing, optimization, pre-turning.

## ABSTRACT

The presented study investigated for the first time the pre-turning performance before the diamond burnishing of AISI 4340 hardened steel under various cutting speeds, feed values, and cutting depths at flood cooling cutting conditions. Multi-objective optimization was conducted to obtain an effective pre-turning process regarding total cost and surface characteristics. The results showed that the pre-turning parameters must be optimized to benefit from diamond burnishing effectively. It was also observed that the diamond burnishing could have been more influential on pre-turned specimens with high surface roughness. Under the bohr-oil-added flood-cutting conditions, the average surface roughness and maximum roughness depth improved by 63.4% and 48.5%, respectively. The most influential parameters for average surface roughness and maximum roughness depth were the feed values with 98.2% and 99.3% contribution ratios, respectively. The Bees algorithm optimized the pre-turning parameters in terms of output parameters. The optimum cutting speed, feed values, and cutting depth levels are 264 m/min, 0.1325 mm/rev, and 0.55 mm, respectively.

**Cite this article as:** Aydın, M., Gökcepınar, Ö. F., & Kalyoncu, M. (2024). Optimization of pre-turning parameters for diamond burnishing of AISI 4340 steel. *J Adv Manuf Eng*, 5(2), 29–36.

## INTRODUCTION

The interest in finishing processes is increasing to improve surface integrity and precisely manufacture parts. Conventional finishing processes such as grinding, honing, and lapping are widely used in applications that require superior surface quality and dimensional accuracy. Roller burnishing (EP) has recently been considered the efficient solution in cases where surface integrity criteria such as surface roughness, compressive residual stresses, and surface microhardness are essential [1]. Also, roller burnishing is a remarkable process for increasing fatigue strength as it generates compressive residual stresses on the surface [2]. This process is performed by a burnishing tool with one or more balls contacting the surface of the workpiece. The burnishing tool or workpiece rotates at a certain speed in the burnishing process. As the tool moves forward, the balls try to burnish the surface by pressing the rough peeks into the micro-gaps. Besides the outer diameters or outer surfaces, the inner diameters of materials with holes inside can also be burnished [3, 4]. Burnishing has significant potential to improve the surface integrity, cost efficiency, and overall quality of products. Burnishing is commonly applied to rotating components that require high-quality standards, such as automotive crankshafts, bearing parts, and axles [5]. In the literature, the roller burnishing method appears in different forms. Some are roller burnishing [6], ball burnishing [7], deep rolling [8], and diamond burnishing [5].

***Corresponding author.**
*E-mail address: maydin@ktun.edu.tr

Published by Yıldız Technical University Press, İstanbul, Türkiye
This is an open access article under the CC BY-NC license (http://creativecommons.org/licenses/by-nc/4.0/).

**Table 1.** Chemical composition of AISI 4340

| Element | C | Si | Mn | P | S | Cr | Ni | Mo | Al |
|---|---|---|---|---|---|---|---|---|---|
| Wt. (%) | 0.41 | 0.19 | 0.65 | 0.007 | 0.005 | 0.7 | 1.7 | 0.24 | 0.039 |

Diamond burnishing is one of the most popular chip-free finishing processes in recent years [9]. Diamond burnishing can modify the surface of materials up to approximately 60 HRC hardness without removing chips. It is a process in which the diamond tip presses the material's surface, forcing plastic deformation. A hard layer is obtained on the surface due to the strain hardening during plastic deformation. Diamond burnishing makes it possible to manufacture parts with low surface roughness and higher surface microhardness compared. The diamond burnishing process is shown schematically in Figure 1.

Numerous studies have demonstrated that roller, ball, and diamond burnishing enhance various materials' surface integrity and geometric tolerances. Some research has also focused on burnishing the inner surfaces of cylinders, investigating the resulting surface integrity [3, 4]. Additionally, various materials have been examined to illustrate improvements in surface integrity, mechanical properties, and fatigue performance, including such as 17–4 PH stainless steel [10], 42CrMo4 [11], AISI 52100 steel [12], AISI 1040 [13], AISI 1045 [14, 15], AISI 1055 [16], Inconel 718 [17, 18], 210Cr12 [19], Mg–SiC metal matrix [20], and 41Cr4 [21]. The findings of these studies reveal that the effectiveness of the burnishing process is highly dependent on the range of burnishing parameters applied, their interactions, the type and hardness of the material being burnished, as well as the lubrication and wear condition of the burnishing head [11].

AISI 4340 is a low alloy-hardenable steel with medium carbon composition (0.38%–0.43%), high toughness and strength (after heat treatment), and is widely used in engineering applications [22]. AISI 4340 is frequently used in the quenched and tempered condition in industry. This steel is extensively used in demanding structural applications such as axles, connecting rods, and transmission gears in the automotive industry, as well as landing gear in the aerospace industry, due to its high strength and toughness [23]. Many researchers are interested in studying the effects of various machining conditions and perspectives for AISI 4340 steel. AISI 4340 is also a material subject to roller and ball burnishing applications [6, 24, 25]. Aviles et al. [26] compared the effect of shot-peening (SP) and low-plasticity burnishing (LPB) on the high cycle fatigue of an AISI 4340, quenched and tempered steel. Compared with the machined specimens, it was concluded that the fatigue limit of the shot-peened specimens increased by 39%, whereas that of the LPB specimens increased by 52%. Aydın and Turkoz (2022) investigated the effect of the roller burnishing process on the surface integrity and fatigue performance of AISI 4340 steel [6]. They found that the surface roughness was reduced from 2.98 to 0.51 µm by roller burnishing. Also, it was stated that the most influential parameter on the fatigue life was the feed rate, with a contribution ratio of 57%. Khodabandeh et al. [27] increased the tensile strength of AISI 4340 material by 6.29% and fatigue strength by 20.71% with hybrid laser-ultrasonic-assisted ball burnishing.

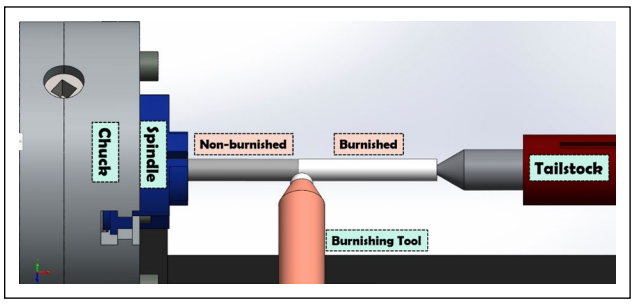


**Figure 1**. Schematic representation of the diamond burnishing process.

This study aims to evaluate the effects of pre-turning parameters on the diamond burnishing of AISI 4340 steel. In this context, multi-objective optimization of the pre-turning process in terms of average surface roughness ($R_a$), maximum roughness depth ($R_z$), material removal rate (RMR), and machining cost was performed. The pre-turning performance in diamond burnishing of AISI 4340 steel was investigated for the first time in the literature. The process variables considered include cutting speed, feed, and cutting depth, each examined at three levels. The $L_9$ orthogonal array designed by Taguchi and Wu [28] was used in the experiments. Variance analysis and regression analysis were used to examine the effects of the input parameters on the performance criteria. Finally, the optimum values of the pre-turning parameters were calculated using the Bees algorithm optimization.

## MATERIAL AND EXPERIMENTAL PROCEDURE

The experimental study used AISI 4340 tempered steel. The material supplier provided the chemical composition of AISI 4340, which is given in Table 1. Three repeated hardness measurements determined the workpiece's hardness as 33 HRC. Rods with a diameter of 24 mm and a length of 100 mm were used in the study.

The experiments were carried out on the DNRdema TTH8 CNC turning machine. The pre-turning of the AISI 4340 was investigated under different turning conditions. Turning and burnishing experiments were conducted in flood-cooling conditions. In all experiments, DNMG150608-GM cemented carbide inserts were used. Experimental setup was given Figure 2. The new insert was used in each experiment. Runout was measured during burnishing and the maximum runout was 0.02 mm. After the pre-turning, diamond burnishing experiments were performed at the 100 m/min burnishing speed, 0.1 mm/rev burnishing feed value, and 0.3 mm burnishing depth by us-

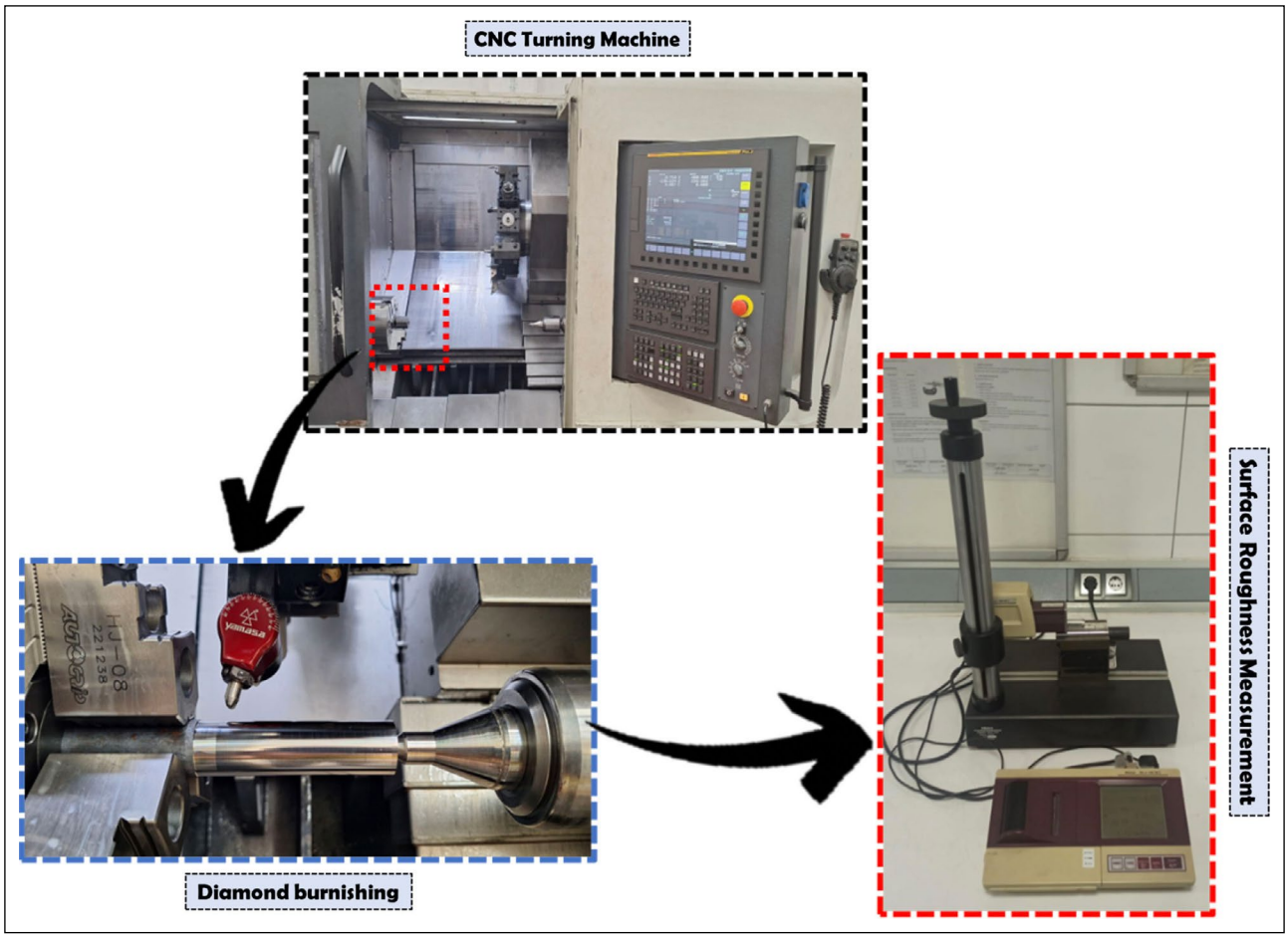


**Figure 2**. Experimental set up.

**Table 2.** Parameters and levels used in pre-turning experiments

| Level Parameter | Cutting speed (m/min) | Feed value (mm/rev) | Cutting depth (mm) |
|---|---|---|---|
| 1 | 200 | 0.1 | 0.5 |
| 2 | 275 | 0.2 | 1.0 |
| 3 | 350 | 0.4 | 1.5 |

ing diamond burnishing tool with 4 mm diameter diamond ball. $R_a$ and $R_z$ were measured after turning and burnishing to show the effect of different pre-turning parameters on burnished AISI 4340. Measurements were performed using the Mitutoyo Surftest SJ - 401 digital roughness tester with three repetitions. The average roughness of these three measurements is presented in the results section. Measurements were made by ISO 4287:1997. The diamond-tipped probe moves at a speed of 0.5 mm/s, and the cut-off length (λc) is set to 0.8 mm for the measurements.

This study's input parameters are cutting speed (m/min), feed value (mm/rev), and cutting depth (mm). Each parameter has three levels, and a Taguchi $L_9$ experimental design was used. The parameters and their levels are shown in Table 2, and the experimental design is shown in Table 3. Pre-turning parameter levels were taken as minimum - median - maximum values in line with the recommendations of the cutting tool supplier.

**Table 3.** Taguchi $L_9$ experimental design

| Experiment | Cutting speed (m/min) | Feed value (mm/rev) | Cutting depth (mm) |
|---|---|---|---|
| 1 | 200 | 0.1 | 0.5 |
| 2 | 200 | 0.2 | 1.0 |
| 3 | 200 | 0.4 | 1.5 |
| 4 | 275 | 0.1 | 1.0 |
| 5 | 275 | 0.2 | 1.5 |
| 6 | 275 | 0.4 | 0.5 |
| 7 | 350 | 0.1 | 1.5 |
| 8 | 350 | 0.2 | 0.5 |
| 9 | 350 | 0.4 | 1.0 |

In this study, statistical analyses were performed on the results of $R_a$ and $R_z$. First, variance analysis (ANOVA) was applied to the output parameters using by Minitab 19 software. In the ANOVA table, the p-value and the contribution of the parameters to the results were interpreted. Regression analyses were then performed. Also, the mathematical equation of RMR and total cost is derived and shown in the results section. Regression analysis created mathematical models for $R_a$ and $R_z$. These models were used in the optimization stage. The Bees algorithm proposed by Pham was used for the multi-objective optimization of the pre-turning process for the burnishing process [29].

Four performance criteria ($R_a$, $R_z$, RMR, and total cost) were given equal weights. A single mathematical model was derived after giving 25% weight to the four mathematical models. So, parameters were optimized using the Bees algorithm, and optimum pre-turning parameter levels were determined.

RMR and total cost were calculated analytically. RMR is calculated as in Eq. 1 [30]. The total cost was calculated as the sum of tool and operation costs. The cost per operation minute and a single insert were 5 and 50 TL, respectively. The processing time was calculated using Eq. 2 [30]. Then, the amount of wear (Eq. 3) in a single pass was calculated using Taylor tool wear equations using Eq. 4 [30]. The tool cost in a single pass was calculated using the amount of wear as in Eq. 5. The operation cost is shown in Eq. 6. The total cost is shown in Eq. 7. In the equations, v, f, d, D0, L, T, n, and C represents cutting speed, feed rate, cutting depth, diameter, length, tool wear, wear constants, respectively.

$$RMR\ (m^3/min) = v * f * d \quad (1)$$

$$T_m = \frac{\pi * D_0 * L}{f * v} \quad (2)$$

$$v * T^n = C \quad (3)$$

$$Tool\ wear\ for\ one\ pass\ (\%)\ (TWOP) = \frac{T_m}{T} * 100 \quad (4)$$

$$Tool\ cost\ for\ one\ pass\ (TL)\ (TCOP) = 50 * TWOP \quad (5)$$

$$Operation\ cost\ for\ one\ pass\ (TL)\ (OCOP) = 5\ TL * T_m \quad (6)$$

$$Total\ cost\ of\ machining = TCOP + OCOP \quad (7)$$

## RESULT AND DISCUSSION

### Experimental Results

The experimental results of pre-turning parameters, $R_a$, $R_z$, material removal rate, and total machining cost, were investigated using a Taguchi $L_9$ experimental design. The influence of input parameters on performance criteria was analyzed in detail. Subsequently, the Analysis of Variance (ANOVA) technique was employed to determine the contribution ratio of the parameters to the results and their significance values. Mathematical modeling was conducted using regression analysis based on the results. Additionally, pre-turning parameters were optimized using multi-objective optimization with the Bees algorithm.

**Table 4.** Results of material removal rate (RMR) and total machining cost per pass

| Exp. | Material removal rate ($mm^3$/min) | Total cost per pass (TL) |
|---|---|---|
| 1 | 10000 | 0.94 |
| 2 | 40000 | 0.46 |
| 3 | 120000 | 0.23 |
| 4 | 27500 | 1.01 |
| 5 | 82500 | 0.51 |
| 6 | 55000 | 0.25 |
| 7 | 52500 | 1.41 |
| 8 | 35000 | 0.71 |
| 9 | 140000 | 0.36 |

RMR and total cost results are given in Table 4. The highest RMR was 2.33 $mm^3$/min in the 9th experiment, while the lowest RMR was 0.17 in the 1st experiment. The lowest total cost per pass was calculated at 0.23 TL in the 3rd experiment, while the highest total cost per pass was 1.41 TL in the 7th experiment. In metal cutting, it is expected that the RMR should be high and the total cost should be low. In this way, an efficient manufacturing process is realized by removing many chips at low costs. So, in multi-objective optimization, RMR is maximized while cost is minimized.

The experimental results of average surface roughness ($R_a$), maximum roughness depth ($R_z$), and decrease rates in $R_a$ and $R_z$ are presented in Table 5, using the Taguchi $L_9$ orthogonal array. $V_c$, f and d represent cutting speed, feed value and cutting depth, respectively. The lowest average surface roughness and maximum roughness depth were obtained at 200 mm/min cutting speed, 0.1 mm/rev feed value, and 0.5 mm cutting depth. In contrast, the highest surface roughness was obtained at 275 m/min cutting speed, 0.4 mm/rev feed

**Table 5.** Average surface roughness ($R_a$) and maximum roughness depth ($R_z$) result in decreased rates after diamond burnishing

| Input parameters | | | After the pre-turning experiments | | After the burnishing experiments | | Decrease rate (%) | Decrease rate (%) |
|---|---|---|---|---|---|---|---|---|
| Vc (m/min) | f (mm/rev) | d (mm) | Average surface roughness ($R_a$) (µm) | Maximum surface depth ($R_z$) (µm) | Average surface roughness ($R_a$) (µm) | Maximum surface depth ($R_z$) (µm) | $R_a$ | $R_z$ |
| 200 | 0.1 | 0.5 | 0.168 | 1.23 | 0.120 | 0.80 | 28.6 | 35.0 |
| 200 | 0.2 | 1.0 | 0.538 | 3.06 | 0.307 | 1.63 | 42.9 | 46.7 |
| 200 | 0.4 | 1.5 | 2.018 | 10.46 | 1.740 | 7.23 | 13.8 | 30.9 |
| 275 | 0.1 | 1.0 | 0.223 | 1.88 | 0.163 | 1.37 | 26.9 | 27.1 |
| 275 | 0.2 | 1.5 | 0.574 | 3.14 | 0.387 | 1.90 | 32.6 | 39.5 |
| 275 | 0.4 | 0.5 | 2.029 | 10.71 | 1.753 | 7.63 | 13.6 | 28.8 |
| 350 | 0.1 | 1.5 | 0.292 | 1.94 | 0.107 | 1.00 | 63.4 | 48.5 |
| 350 | 0.2 | 0.5 | 0.720 | 3.57 | 0.510 | 2.23 | 29.2 | 37.5 |
| 350 | 0.4 | 1.0 | 1.728 | 9.90 | 1.557 | 7.40 | 9.9 | 25.3 |

**Figure 3**. Diamond burnished specimens.

value, and 0.5 mm cutting depth. Thus, a 168% reduction was achieved by only changing pre-turning parameter levels. Like the literature, regardless of cutting depth, the surface roughness increased with increasing feed value at the same cutting speed [31]. The lowest in $R_a$ and $R_z$ values were 0.168 µm and 1.23 µm, respectively. The highest in $R_a$ and $R_z$ values were 2.029 µm and 10.71 µm, respectively.

The lowest surface roughness occurred at the lowest cutting speed, feed value, and cutting depth. After the burnishing process, all surface roughness was decreased as expected. It was observed that the rates of decrease in surface roughness after burnishing were affected by varying the pre-turning parameters. It shows the importance of selecting the pre-turning parameters prior to burnishing. The lowest decrease rate in in $R_a$ and $R_z$ were 9.9% and 25.3%, respectively. The decrease rates were generally lower in the experiments with higher surface roughness after pre-turning (e.g., 3$^{rd}$, 6$^{th}$, and 9$^{th}$ experiments). Roller burnishing can be advantageous, but it is easy to see that it is less effective on parts with very high roughness. One of the main reasons for this result is the formation of surface roughness at depths inaccessible by the diamond tip. In addition, the cutting temperature increases as the feed rate increases. The material's plastic deformation ability may be reduced because it cools and hardens after high cutting temperatures. This mechanism may also be a reason for the decrease in roller burnishing performance. The highest decrease rate of 63.4% occurred in pre-turned specimens with a cutting speed of 350 mm/min, a feed rate of 0.1 mm/rev, and a cutting depth of 1.5 mm. The results conclude that the specimens should be prepared with optimum pre-turning conditions to get maximum benefit from the burnishing process. In our previous study, we investigated the effects of roller burnishing of hardened AISI 4340 steel (42 HRC) on surface integrity and axial fatigue performance. Similar to this study, improvements in surface roughness ranging from 9% to 78% were observed [6]. In addition, the improvement in surface roughness in another study supports the results of this study [26]. Diamond-burnished specimens after pre-turning are shown in Figure 3.

**Analysis of Variance (ANOVA) and Regression Analysis**

ANOVA was conducted to elucidate the effects of pre-turning parameters on the surface characteristic of burnished AISI 4340 steels. The ANOVA tables provide insights into the parameters' p-values and contribution ratios. The p-value, also called the significance measure, indicates statistical significance when small (typically less than 0.05), suggesting a statistically significant effect of the input parameters [32]. However, it is crucial to note that the p-value should not be the sole measure of evidence in a scientific study. The contribution ratio quantifies the proportion of total variation in the response variable attributable to a specific independent variable. A high contribution ratio indicates the independent parameter's strong influence on the outcome, whereas a low contribution ratio signifies a weaker influence.

The ANOVA table for the $R_a$ for pre-turning is given in Table 6. The ANOVA tables were generated by using Minitab 19 software. Only the p-value of the feed value in the table is less than 0.05. This result shows that the feed value has a dominant effect on the $R_a$ and $R_z$. This result is similar to the literature. Similarly, in the study of Boozarpoor et al. [24], feed rate was the most effective parameter in roller burnishing for AISI 4340 material. It was thought that the parameter levels selected may be responsible for this result. However, the parameter levels were selected within the range given by the tool manufacturer. Therefore, the dominance of the feed value did not occur after selecting an extreme parameter level. The contribution ratio of the feed value on the average surface roughness was calculated as 98.25%. The cutting depth and cutting speed came in second and third, with contribution ratios of 0.78% and 0.04%, respectively. The error ratio in the ANOVA analysis was calculated as 0.92%. A similar observation was seen in the ANOVA table of $R_z$ in pre-turning. The contribution ratio of the feed value on the maximum roughness depth was calculated as 99.38%. The cutting depth and cutting speed came in second and third, with contribution ratios of 0.41% and 0.13%, respectively. The error ratio in the ANOVA analysis was calculated as 0.41%. The dominance of feed

**Table 6.** ANOVA tables for $R_a$ and $R_z$ for pre-turning and after diamond burnishing

| Source | SS | DF | f-value | p-value | Cont.% | Remarks |
|---|---|---|---|---|---|---|
| $R_a$ in pre-turning | | | | | | |
| Cutting speed (m/min) | 0.002 | 2 | 0.04 | 0.957 | 0.04 | Non-significant |
| Feed value (mm/rev) | 4.755 | 2 | 106.24 | 0.009 | 98.25 | Significant |
| Cutting depth (mm) | 0.037 | 2 | 0.84 | 0.542 | 0.78 | Non-significant |
| Error | 0.044 | 2 | | | 0.92 | |
| Total | 4.839 | 8 | | | 100.00 | |
| $R_z$ in pre-turning | | | | | | |
| Cutting speed (m/min) | 0.166 | 2 | 0.31 | 0.762 | 0.13 | Non-significant |
| Feed value (mm/rev) | 128.1 | 2 | 240.05 | 0.004 | 99.38 | Significant |
| Cutting depth (mm) | 0.104 | 2 | 0.2 | 0.836 | 0.08 | Non-significant |
| Error | 510.6 | 2 | | | 0.41 | |
| Total | 128.91 | 8 | | | 100.00 | |
| $R_a$ after burnishing | | | | | | |
| Cutting speed (m/min) | 0.003 | 2 | 0.18 | 0.846 | 0.09 | Non-significant |
| Feed value (mm/rev) | 4.129 | 2 | 192.6 | 0.005 | 98.88 | Significant |
| Cutting depth (mm) | 0.021 | 2 | 0.99 | 0.501 | 0.51 | Non-significant |
| Error | 0.021 | 2 | | | 0.51 | |
| Total | 4.176 | 8 | | | 100.00 | |
| $R_z$ after burnishing | | | | | | |
| Cutting speed (m/min) | 0.283 | 2 | 2.89 | 0.257 | 0.39 | Non-significant |
| Feed value (mm/rev) | 71.48 | 2 | 728.31 | 0.001 | 99.40 | Significant |
| Cutting depth (mm) | 0.046 | 2 | 0.48 | 0.677 | 0.07 | Non-significant |
| Error | 0.098 | 2 | | | 0.14 | |
| Total | 71.915 | 8 | | | 100.00 | |

SS: Sum of squares; DF: Degree of freedom; F-value: Fisher test; p: Probability; Cont.%: Percentage contribution.

value continued after burnishing. Similar results can be easily seen in the ANOVA tables after burnishing.

This study used regression analysis to create mathematical models for $R_a$ and $R_z$. The R-square values of the mathematical equations, ranging from 0 to 1, were obtained. A higher R-square value indicates that the input variables predict the output variable more accurately. The regression models of $R_a$ and $R_z$ are presented in Eqs. 8 and 9. An equally weighted (0.25) multi-objective mathematical model, given in Eq. 10, was derived using all the individual models. The optimal pre-turning parameter levels were determined using the Bees Algorithm.

$$\text{Average Surface Roughness } (R_a) = -0.7547+0.007159*v-1.5*f-0.07474*d-0.000008*v*v+14.87*f*f+0.2614*d*d-0.003637*v*f-0.001949*v*d \quad (8)$$

$$\text{Maximum Roughness Depth } (Rz) = -3.664+0.03396*v-12.22*f+1.420*d-0.000047*v*v+68.96*f*f-0.1919*d*d-0.005911*v*f-0.004648*v*d \quad (9)$$

$$\text{Weighed objective function} = (0.25*R_a)*(0.25*R_z)*(0.25*\text{Total Cost})*\left(\frac{0.25}{RMR}\right) \quad (10)$$

**Multi-Objective Optimization by the Bees Algorithm**

The optimal pre-turning parameters obtained using the Bees Algorithm are the cutting speed of 264 m/min, feed value of 0.1325 mm/rev, and cutting depth of 0.55 mm when evaluating average surface roughness, maximum roughness depth, material removal rate, and total machining cost. The convergence graph of the optimization result is given in Figure 4. It is seen that the algorithm ultimately converges after 400 iterations.

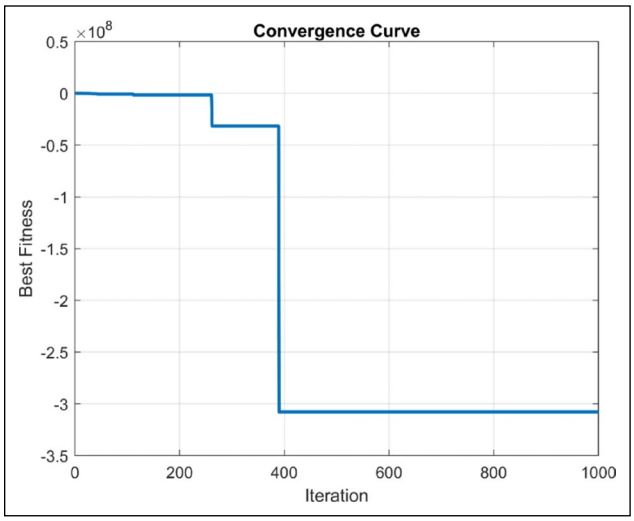


**Figure 4**. The convergence curve resulted from multi-objective optimization.

## CONCLUSION

This study presents the pre-turning performance of burnished AISI 4340 hardened steels using three different cutting speeds, feed values, and cutting depth. Next, a multi-objective weighted optimization was conducted to minimize the average surface roughness, maximum roughness depth, and material total machining cost and to maximize the material removal rate using the Bees algorithm. The results obtained from the experimental study can be summarized as follows:

1 The burnishing process after pre-turning was effective on all specimens. Average surface roughness decreased by a maximum of 63.4% and a minimum of 9.9% after pre-turning. Also, the maximum roughness depth decreased by a maximum of 48.5 and a minimum of 25.3 after pre-turning.
2 The feed value is most effective in influencing average surface roughness and maximum roughness depth, with contribution ratios of 98.2% and 99.3%, respectively.
3 The presented study has shown that choosing pre-turning parameters before the burnishing of AISI 4340 steel is important, especially regarding surface characteristics.
4 The optimal pre-turning parameters obtained using the Bees Algorithm are a cutting speed of 264 m/min, a feed value of 0.132 mm/rev, and a cutting depth of 0.554 mm when evaluating average surface roughness, maximum roughness depth, material removal rate, and total machining cost.

**Acknowledgements**

The work presented in this article is supported by Konya Technical University Research Project Unit (BAP) with Project Number 232010037. We would like to thank Konya Technical University.

**Data Availability Statement**

The authors confirm that the data that supports the findings of this study are available within the article. Raw data that support the finding of this study are available from the corresponding author, upon reasonable request.

**Author's Contributions**

Mevlüt Aydın: Carried out experiments and writing.

Ömer Faruk Gökçepınar: Carried out experiments and writing.

Mete Kalyoncu: Carried out optimization procedures and algorithms.

**Conflict of Interest**

The authors declared no potential conflicts of interest with respect to the research, authorship, and/or publication of this article.

**Use of AI for Writing Assistance**

Not declared.

**Ethics**

There are no ethical issues with the publication of this manuscript.

## REFERENCES

[1] El-Axir, M. H. (2000). An investigation into roller burnishing. *International Journal of Machine Tools and Manufacture*, *40*(11), 1603–1617. [CrossRef]

[2] Priyadarsini, C., Ramana, V. S. N. V., Prabha, K. A., & Swetha, S. (2019). A review on ball, roller, low plasticity burnishing process. *Materials Today: Proceedings*, *18*, 5087–5099. [CrossRef]

[3] Babu, P. R., Prasad, T. S., Raju, A. V. S., & Babu, A. J. (2009). Effect of internal roller burnishing on surface roughness and surface hardness of mild steel. *Journal of Scientific & Industrial Research*, *68*, 29–31.

[4] Stalin John, M. R., Balaji, B., & Vinayagam, B. K. (2017). Optimisation of internal roller burnishing process in CNC machining center using response surface methodology. *Journal of the Brazilian Society of Mechanical Sciences and Engineering*, *39*(10), 4045–4057. [CrossRef]

[5] Korzynski, M., Lubas, J., Swirad, S., & Dudek, K. (2011). Surface layer characteristics due to slide diamond burnishing with a cylindrical-ended tool. *Journal of Materials Processing Technology, 211*(1), 84–94. [CrossRef]

[6] Aydın, M., & Türköz, M. (2022). A study on the effect of the roller burnishing process on the axial fatigue performance and surface integrity of AISI 4340 steel. *Journal of the Brazilian Society of Mechanical Sciences and Engineering, 44*(6), 1–16. [CrossRef]

[7] Livatyali, H., Has, E., & Türköz, M. (2020). Prediction of residual stresses in ball burnishing TI6AL4V thin sheets. *International Journal of Advanced Manufacturing Technology, 110*(3–4), 1083–1093. [CrossRef]

[8] Muñoz-Cubillos, J., Coronado, J. J., & Rodríguez, S. A. (2017). Deep rolling effect on fatigue behavior of austenitic stainless steels. *International Journal of Fatigue, 95*, 120–131. [CrossRef]

[9] Huuki, J., & Laakso, S. V. A. (2017). Surface improvement of shafts by the diamond burnishing and ultrasonic burnishing techniques. *International Journal of Machining and Machinability of Materials, 19*(3), 246–259. [CrossRef]

[10] Sachin, B., Narendranath, S., & Chakradhar, D. (2018). Experimental evaluation of diamond burnishing for sustainable manufacturing. *Materials Research Express, 5*(10), Article 106514. [CrossRef]

[11] Zaghal, J., Molnár, V., & Benke, M. (2023). Improving surface integrity by optimizing slide diamond burnishing parameters after hard turning of 42CrMo4 steel. *International Journal of Advanced Manufacturing Technology, 128*(5–6), 2087–2103. [CrossRef]

[12] Ouahiba, T., Hamid, H., Selma, B., & Laouar, L. (2024). Multi-objective optimization of slide diamond burnishing parameters for enhanced fatigue resistance of AISI 52100 steel. *Journal of the Brazilian Society of Mechanical Sciences and Engineering, 46*(8), Article 451. [CrossRef]

[13] Cobanoglu, T., & Ozturk, S. (2015). Effect of burnishing parameters on the surface quality and hardness. *Proceedings of the Institution of Mechanical Engineers, Part B: Journal of Engineering Manufacture, 229*(2), 286–294. [CrossRef]

[14] Saldaña-Robles, A., Plascencia-Mora, H., Aguilera-Gómez, E., Saldaña-Robles, A., Marquez-Herrera, A., & Diosdado-De la Peña, J. A. (2018). Influence of ball-burnishing on roughness, hardness and corrosion resistance of AISI 1045 steel. *Surface and Coatings Technology, 339*, 191–198. [CrossRef]

[15] Rodríguez, A., López de Lacalle, L. N., Celaya, A., Lamikiz, A., & Albizuri, J. (2012). Surface improvement of shafts by the deep ball-burnishing technique. *Surface and Coatings Technology, 206*(11–12), 2817–2824. [CrossRef]

[16] Okada, M., Suenobu, S., Watanabe, K., Yamashita, Y., & Asakawa, N. (2015). Development and burnishing characteristics of roller burnishing method with rolling and sliding effects. *Mechatronics, 29*, 110–118. [CrossRef]

[17] López de Lacalle, L. N., Lamikiz, A., Sánchez, J. A., & Arana, J. L. (2007). The effect of ball burnishing on heat-treated steel and Inconel 718 milled surfaces. *The International Journal of Advanced Manufacturing Technology, 32*, 958–968. [CrossRef]

[18] Sequera, A., Fu, C. H., Guo, Y. B., & Wei, X. T. (2014). Surface integrity of Inconel 718 by ball burnishing. *Journal of Materials Engineering and Performance, 23*(9), 3347–3353. [CrossRef]

[19] Qiao, Y., Chen, H., Qi, K., & Guo, P. (2020). Research on mechanical properties of 210cr12 shaft surface processed with rolling. *Coatings, 10*(7), Article 611. [CrossRef]

[20] Arun, K. R., & Stalin, P. M. R. (2021). Optimization of external roller burnishing process on magnesium silicon carbide metal matrix composite using response surface methodology. *Journal of the Brazilian Society of Mechanical Sciences and Engineering, 43*(7), 1–12. [CrossRef]

[21] Maximov, J. T., Duncheva, G. V., Anchev, A. P., Dunchev, V. P., & Ichkova, M. D. (2020). Improvement in fatigue strength of 41Cr4 steel through slide diamond burnishing. *Journal of the Brazilian Society of Mechanical Sciences and Engineering, 42*(4), 1–20. [CrossRef]

[22] Bag, R., Panda, A., Sahoo, A. K., & Kumar, R. (2020). A comprehensive review on AISI 4340 hardened steel: Emphasis on industry ımplemented machining settings, implications, and statistical analysis. *International Journal of Integrated Engineering, 12*(8), 61–82. [CrossRef]

[23] de Souza, M. F., Serrão, L. F., Pardal, J. M., Tavares, S. S. M., & Fonseca, M. C. (2022). Tempering influence on residual stresses and mechanical properties of AISI 4340 steel. *International Journal of Advanced Manufacturing Technology, 120*(1–2), 1123–1134. [CrossRef]

[24] Boozarpoor, M., & Elyasi, M. (2018). An investigation of the surface quality of burnished AISI 4340 steel. *Proceedings of the Institution of Mechanical Engineers, Part E: Journal of Process Mechanical Engineering, 232*(3), 299–313. [CrossRef]

[25] Cammett, J. T., & Prevey, P. S. (2015). Fatigue strength restoration in corrossion pitted 4340 alloy steel via low plasticity Burnishing, Proceedings of the National Turbine Engine High Cycle Fatigue (HCF) Conference April 14-16, Monterey, CA, 2003.

[26] Avilés, A., Avilés, R., Albizuri, J., Pallarés-Santasmartas, L., & Rodríguez, A. (2019). Effect of shot-peening and low-plasticity burnishing on the high-cycle fatigue strength of DIN 34CrNiMo6 alloy steel. *International Journal of Fatigue, 11*, 338–354. [CrossRef]

[27] Khodabandeh, A., Sayadi, D., Rajabi, S., Khosrojerdi, M., Khajehzadeh, M., & Razfar, M. R. (2024). Surface integrity and fatigue behavior of AISI 4340 steel after hybrid laser-ultrasonic assisted ball burnishing process. Proceedings of the Institution of Mechanical Engineers, Part C: *Journal of Mechanical Engineering Science, 238*(15), 7607–7626. [CrossRef]

[28] Taguchi, G., & Wu, Y. (1979). *Introduction to offline quality control*. Central Japan Quality Control Assoc.

[29] Pham, D. T., Ghanbarzadeh, A., Koç, E., Otri, S., Rahim, S., & Zaidi, M. (2006). The bees algorithm—a novel tool for complex optimisation problems. *Intelligent production machines and systems* (pp. 454–459). Elsevier Science Ltd. [CrossRef]

[30] Groover, M. P. (2010). *Fundamentals of modern manufacturing: materials, processes, and systems*. John Wiley & Sons.

[31] Aggarwal, A., Singh, H., Kumar, P., & Singh, M. (2009). Optimizing feed and radial forces in CNC machining of P-20 tool steel through Taguchi's parameter design approach. *Indian Journal of Engineering & Materials Sciences, 16*, 23–32.

[32] St, L., & Wold, S. (1989). Analysis of variance (ANOVA). *Chemometrics and Intelligent Laboratory Systems, 6*(4), 259–272. [CrossRef]